Impact of cross phase modulation and cross polarization modulation in 33 Gbaud PM-16QAM signals in legacy OOK WDM systems

Author One,[1] Author Two,[2,*] and Author Three[2,3]

[1] *Peer Review, Publications Department, The Optical Society (OSA), 2010 Massachusetts Avenue NW, Washington, DC 20036, USA*
[2] *Publications Department, The Optical Society (OSA), 2010 Massachusetts Avenue NW, Washington, DC 20036, USA*
[3] *Currently with the Department of Electronic Journals, The Optical Society (OSA), 2010 Massachusetts Avenue NW, Washington, DC 20036, USA*
[*] *opex@osa.org*

Abstract: LaTeX manuscripts submitted to OSA journals as of 30 May 2018 may use these instructions and this new single-column universal template format. Note that the final publishing format of OSA journals is not changing at this time, and authors will still need to adhere to article-length restrictions based on the final publishing format (which for some journals is two columns). Authors of Optics Letters articles and Optica letters and memoranda should continue using the legacy template for an accurate length check. Please note that OSA is no longer using OCIS codes.

1. Introduction

To fulfill the ever-growing bandwidth demands in optical networks, operators are interested in a cost efficient and smooth upgrade of their legacy on/off keying (OOK) channels to higher modulation formats in wavelength division multiplexing (WDM) systems. Such systems are typically called hybrid systems and have been studied by several research groups [1–6].

In [1], a 10 Gbaud polarization multiplexing differential quadrature phase shift keying (PM-DQPSK) channel performance is simulated with 4 neighboring non-return-to-zero (NRZ) OOK channels in a non-zero dispersion shifted fiber (NZ-DSF). Their results shown that the performance of the PM-DQPSK channel is worst when the state of polarization (SOP) of the OOK neighboring channels is set to 0 deg and 90 deg (relative to the X polarization of the PM-DQPSK channel), and best when the SOP is 45 deg. It is important to note that a polarization controller was used to minimize the bit error rate (BER) at each polarization, therefore, polarization mixing was avoided. In [2], a 28 Gbaud coherent PM-QPSK channel performance was simulated in presence of 2 OOK neighbors using standard single mode fiber (SSMF) and full inline dispersion compensation (DC), their results shown that the performance of the coherent channel was not dependent of the SOP of the neighboring channels in contrast to [1]. In [3], a numerical simulation and experimental setup was investigated for a 40 Gbaud return-to-zero (RZ) PM-DQPSK/D8PSK in an hybrid system with SSMF and full inline DC. Their simulation results shown that the best performance is achieved when the SOP of the OOK channels is 0 deg or 90 deg and the worst performance is for 45 deg (even after BER optimization with polarization controller). Their experimental results lie between those of the simulations since, in the experiment, the SOP of the OOK channels is uncontrolled and gets further randomized during transmission. This result disagrees with publications [1, 2] and the authors suggests that further studies are necessary. In [4], a theoretical analysis from the Manakov equation is performed and it shows that cross polarization modulation (XPolM) effects are minimum when the SOP of the OOK channels is 0 deg or 90 deg and maximum when is 45 deg. A simulation with a 28 Gbaud coherent PM-QPSK

channel with 6 OOK neighbors using random and 0 deg SOP for the neighbors agrees with the theoretical analysis.

The studies performed in the literature, have been focused in polarization multiplexing differential and coherent phase shift keying (PM (D)xPSK) modulation formats and shown that the performance is severely impacted by cross phase modulation (XPM) and XPolM. As higher modulation formats will be needed to fulfill the bandwidth demands in hybrid systems, in this paper we study and theoretically clarify the effects of XPM and XPolM on a PM-16QAM channel. In section 2, we show a theoretical analysis of XPM and XPolM based on [7, 8], and we discuss some relevant comments related to the case of PM-16QAM. Section 3 and 4 shows the simulation setup and the results of different simulated scenarios in hybrid systems, here we show the agreement of theory with simulations and show the impact of the constant modulus algorithm (CMA) to overcome the effects of XPolM.

2. Theoretical Analysis

Starting from the Manakov equation and following the derivation presented by Karlsson and Sunnerud in [7]:

$$\frac{d\boldsymbol{E}}{dz} = i(\beta + \gamma' \boldsymbol{E}^{+}\boldsymbol{E})\boldsymbol{E} \tag{1}$$

where $\boldsymbol{E} = [\boldsymbol{E}_x; \boldsymbol{E}_y]$ is the electric-field vector, $\beta(\omega_0 - i\partial/\partial t)$ is the dispersion operator, and the non-linear coefficient $\gamma' = 8\gamma/9$ enters with the averaging factor 8/9 due to the polarization averaging [7, 9, 10]. Note that we will drop the prime on γ from now on. The notation $\boldsymbol{E}^{+}$ indicates conjugate transpose, so that $\boldsymbol{E}^{+}\boldsymbol{E} = |\boldsymbol{E}|^2$ is the scalar optical power.

When a single field $\boldsymbol{E}$ is considered, the two complex vector components define the polarization state of the wave. For a continuous wave (CW) field, the polarization state and the amplitude will not change and we will only observe the phase evolution according to self phase modulation (SPM) $\boldsymbol{E}(z) = \boldsymbol{E}(0)exp(i\gamma\,|\boldsymbol{E}(0)|^2\, z$, but when considering several wavelengths with colliding pulses, we can find the polarization dependence at each wavelength.

By substitution of the field $\boldsymbol{E}$ by two fields at different frequencies $\boldsymbol{E} = \boldsymbol{a}exp(i\omega_a t) + \boldsymbol{b}exp(i\omega_b t)$ with non-overlapping spectra, they can be modeled as two coupled equations with center frequencies ω_a and ω_b as in [7, 11–14]:

$$\frac{\partial \boldsymbol{a}}{\partial z} = i(\beta_a + \gamma \boldsymbol{a}^{+}\boldsymbol{a} + \gamma \boldsymbol{b}^{+}\boldsymbol{b})\boldsymbol{a} + \gamma(\boldsymbol{b}^{+}\boldsymbol{a})\boldsymbol{b} \tag{2}$$

$$\frac{\partial \boldsymbol{b}}{\partial z} = i(\beta_b + \gamma \boldsymbol{b}^{+}\boldsymbol{b} + \gamma \boldsymbol{a}^{+}\boldsymbol{a})\boldsymbol{b} + \gamma(\boldsymbol{a}^{+}\boldsymbol{b})\boldsymbol{a} \tag{3}$$

The first term on the right-hand side contains the dispersion operators $\beta_{a,b}$, the second term models the SPM and the third and fourth terms model the XPM and XPolM respectively. In (2) and (3), only the fourth term is polarization dependent and is influenced by the relative polarization of the vector fields $\boldsymbol{a}$ and $\boldsymbol{b}$. In order to observe and quantify the the polarization dependence, we reformulate the problem in terms of the coherency matrix, which for the field $\boldsymbol{a}$ is defined as:

$$\boldsymbol{S}_a = \boldsymbol{a}\boldsymbol{a}^{+} = \begin{pmatrix} \boldsymbol{a}_x\boldsymbol{a}_x^{*} & \boldsymbol{a}_x\boldsymbol{a}_y^{*} \\ \boldsymbol{a}_y\boldsymbol{a}_x^{*} & \boldsymbol{a}_y\boldsymbol{a}_y^{*} \end{pmatrix} = \frac{1}{2}(s_{0a}\sigma_0 + s_a \cdot \boldsymbol{\sigma}) \tag{4}$$

where $\boldsymbol{a} = \begin{pmatrix} \boldsymbol{a}_x \\ \boldsymbol{a}_y \end{pmatrix}$. Here we also use the Pauli spin matrices that are defined as:

$$\sigma_0 = \begin{pmatrix} 1 & 0 \\ 0 & 1 \end{pmatrix} \quad \sigma_1 = \begin{pmatrix} 1 & 0 \\ 0 & -1 \end{pmatrix} \quad \sigma_2 = \begin{pmatrix} 0 & 1 \\ 1 & 0 \end{pmatrix} \quad \sigma_3 = \begin{pmatrix} 0 & -i \\ i & 0 \end{pmatrix}$$

and the vector $\boldsymbol{\sigma} = (\sigma_1, \sigma_2, \sigma_3)$. The stokes vector for the field $\boldsymbol{a}$ is defined by $\boldsymbol{s}_a = \boldsymbol{a}^+\boldsymbol{\sigma}\boldsymbol{a}$, and the optical power $P_a = s_{a,0} = \boldsymbol{a}^+\sigma_0\boldsymbol{a} = \boldsymbol{a}^+\boldsymbol{a}$. Note that the coherency matrix contains information about the optical power and polarization, but not the optical phase that will be shown later. By using (2), we can show the governing equation for the coherency matrix as:

$$\frac{\partial S_a}{\partial z} = \boldsymbol{a'}\boldsymbol{a}^+ = i\gamma[(\boldsymbol{b}^+\boldsymbol{a})\boldsymbol{b}\boldsymbol{a}^+ - \boldsymbol{a}\boldsymbol{b}^+(\boldsymbol{a}^+\boldsymbol{b})]. \tag{5}$$

Note that since the bracketed factors in (5) are scalar, we may put them between the vectors, e.g., $\boldsymbol{a}\boldsymbol{b}^+(\boldsymbol{a}^+\boldsymbol{b}) = \boldsymbol{a}(\boldsymbol{a}^+\boldsymbol{b})\boldsymbol{b}^+ = S_aS_b$. Consequently, we can write the nonlinear evolution of the coherency matrix as:

$$\frac{\partial S_a}{\partial z} + i\gamma\{S_a, S_b\} = 0 \tag{6}$$

$$\frac{\partial S_b}{\partial z} + i\gamma\{S_b, S_a\} = 0 \tag{7}$$

Where $\{S_a, S_b\} = S_aS_b - S_bS_a$ denotes the commutator. By using the rules of quaternion calculus [15], or Pauli matrix calculus [16], we can show that:

$$\{S_a, S_b\} = \frac{i}{2}(\boldsymbol{s}_a \times \boldsymbol{s}_b) \cdot \boldsymbol{\sigma} \tag{8}$$

and thus, (6)-(7) are equivalent to:

$$\frac{\partial P_a}{\partial z} = 0 \tag{9}$$

$$\frac{\partial P_b}{\partial z} = 0 \tag{10}$$

$$\frac{\partial \boldsymbol{s}_a}{\partial z} = \gamma \boldsymbol{s}_a \times \boldsymbol{s}_b \tag{11}$$

$$\frac{\partial \boldsymbol{s}_b}{\partial z} = \gamma \boldsymbol{s}_b \times \boldsymbol{s}_a \tag{12}$$

This model was originally derived in [11] and shows the XPolM. Equations (11)-(12) can be solved by noticing that the total Stokes vector $\boldsymbol{s}_{tot} = \boldsymbol{s}_a + \boldsymbol{s}_b$ is constant and the solution can be written as:

$$\boldsymbol{s}_{a,b}(z) = exp(\gamma z \boldsymbol{s}_{tot}\times)\boldsymbol{s}_{a,b}(0) \tag{13}$$

where $exp(\gamma z \boldsymbol{s}_{tot}\times)$ is the rotation operator for rotating an angle $\gamma z\,|\boldsymbol{s}_{tot}|$ around the vector $\boldsymbol{s}_{tot}$. Consequently, the XPolM will cause the Stokes vectors to rotate around their sum. In the case of an hybrid system, we will be interested in the polarization of our coherent channel where the SOP will rotate around the total Stokes vector during propagation in the nonlinear fiber. Furthermore, we will have the influence of walk off and pattern dependency contributing to this effect.

To get an equation for the absolute phase of the fields, we define the absolute phase of field a as:

$$\frac{\partial \phi_a}{\partial z} = \frac{i(\boldsymbol{a'}^+\boldsymbol{a} - \boldsymbol{a}^+\boldsymbol{a'})}{2\boldsymbol{a}^+\boldsymbol{a}} \tag{14}$$

After using(2)-(3), and $(\boldsymbol{b}^+\boldsymbol{a})\boldsymbol{b} = \boldsymbol{b}(\boldsymbol{b}^+\boldsymbol{a}) = S_b\boldsymbol{a} = (P_b + \boldsymbol{s}_b\cdot)\boldsymbol{a}/2$, we obtain:

$$\frac{\partial \phi_a}{\partial z} = \gamma\left(P_a + \frac{3P_bP_a + \boldsymbol{s}_a \cdot \boldsymbol{s}_b}{2P_a}\right) \tag{15}$$

In this expression the first term is the SPM and the remaining terms are the XPM. We can observe that the last term has a polarization dependent part but it should not be confused with the XPolM as described by equations (11)-(12). The XPolM will be visible in the Poincare sphere while the XPM will be visible in the constellation diagram. We may note that the XPM, has a 3-dB polarization dependence, as it goes between $2P_b$ when the a and b fields are co-polarized, and P_b, when the field are orthogonally polarized. This phase variation will be present in our coherent channel constellation diagram and we will observe this behaviour when simulating the PM-16QAM channel in our hybrid system.

3. Simulation setup

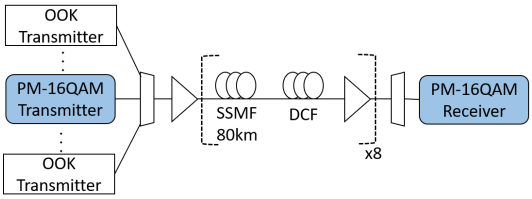

Fig. 1. Simulation Setup.

The setup for the numerical simulations using Matlab® is shown in Fig. 1. It consists of a variable number of 10 Gb/s NRZ OOK channels neighboring a 33 Gbaud PM-16QAM. The coherent channel is Gray codded and shaped with a root-raised cosine (RRC) filter with 0.2 roll-off. Each data channel is generated by a decorrelated pseudo random bit sequence (PRBS) and modulated in an ideal mach-zehnder modulator (MZM), a total of 32,768 symbols were simulated at 64 samples per symbol. The operation wavelength of the PM-16QAM signal is at 1550 nm and the channel spacing is 50 GHz, we also consider a guard band channel around the coherent channel. The link consists of 8 spans with 80 km SSMF with ideal dispersion and loss compensation after each span. The attenuation in SSMF is 0.2 dB/km, the dispersion is 17 ps/nm-km and the non-linear coefficient is 1.37 $W^{-1}km^{-1}$. The erbium doped fiber amplifier (EDFA) noise figure (NF) is 5 dB and the dispersion compensating fiber (DCF) has 0 dB/km loss and 0 $W^{-1}km^{-1}$ non-linear coefficient. Fiber propagation is solved by using the Manakov model and neglecting polarization mode dispersion (PMD). At the receiver a RRC filter with the same characteristics as in the transmitter is used to filter the PM-16QAM channel. The digital signal processing (DSP) algorithm to recover the in-phase and quadrature components of each polarizations includes the constant modulus algorithm (CMA) for polarization recovery and the decision driven least mean squares (DD-LMS) algorithm for phase estimation. The BER is minimized by comparing the transmitted constellation with all the phase and polarization combinations in the received constellation.

4. Simulation results

To study the effects of XPM and XPolM on a PM-16QAM channel in hybrid systems, we first performed simulations with the SOP of the neighboring OOK channels parallel to each other and we rotate the SOP of the OOK channels by an angle α relative to the X polarization of the PM-16QAM channel. Fig. 2 shows the SOP for a PM-16QAM signal and an OOK signal in X Polarization, Y Polarization and +45 deg polarization. From the transmitter, the PM-16QAM signal has 52 SOP around the Poincare sphere. On the other hand, the OOK channel has a single SOP around the equator of the sphere where is linearly polarized. The Poincare sphere and the

SOP of the PM-16QAM signal will help us to visualize the effect of XPolM on the channel under test.

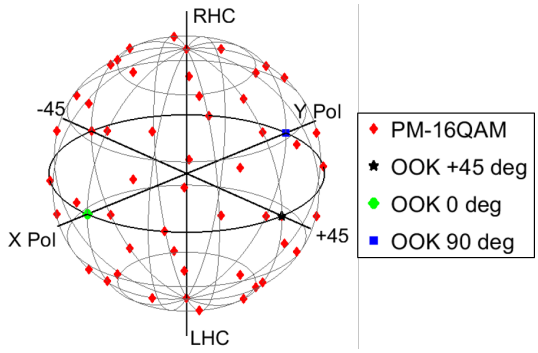

Fig. 2. SOP of PM-16QAM signal. SOP of the OOK signal. X Polarization, Y Polarization, Linear -45 Polarization, linear +45 Polarization, Left Hand Circular (LHC), Rigth Hand Circular (RHC).

Fig. 3 shows the performance simulation of the PM-16QAM in function of SNR and input power per channel. In this simulation we consider that the OOK and PM-16QAM channels have the same optical power and we increase the power of all channels simultaneously. Our simulation results shown that the performance of each polarization of the 16QAM signal is most degraded when the SOPs of the OOK channels are parallel to it and less degraded when are orthogonal to it. For high optical powers, the total nonlinear penalty is ~3 dB higher for the parallel 16QAM signal than for the orthogonal signal. Also, when α=45 deg, the difference between the minimum penalty is ~1.7 dB. The 3 dB difference corresponds to the XPM polarization dependent term as shown in (15). The XPM becomes twice as large for co-polarized signals than for orthogonal signals. The 1.7 dB difference between the orthogonal polarization and the XPM term affecting both polarizations equally [4, 7].

To understand this behavior, it is useful to visualize the Poincare sphere with the SOP of the received PM-16QAM signal. Fig. 4 shows the SOP at the transmitter (red diamonds) and receiver side (blue dots) before and after passing by the CMA polarization recovery stage in the DSP. The received constellation of the X and Y polarizations in the transmitter is also shown. To highlight the nonlinear impairments and for a better visualization, we have neglected the Amplified Spontaneous Emission (ASE) in the amplifiers.

From Fig. 4, it is easy to visualize the effects of XPolM and XPM. The Poincare sphere shows the SOP rotation of our PM-16QAM channel around the sum of the total Stokes vector. The dominant SOP is the one of the OOK channels and the rotation is observed around the SOP of the OOK neighbors. For cases "a" and "b", where the OOK channels have α=0 deg, the CMA algorithm has no effect in the constellation diagrams or SOP in the Poincare sphere so no improvement is observed after polarization recovery. The constellation diagram, shows the polarization dependent contribution to XPM that affects the nonlinear phase noise of the parallel polarization in our 16QAM signal. From (15) we can see that the phase noise contribution will be twice as large for the X Polarization than for the Y Polarization, this result can also be observed from the SNR power penalty in Fig. 3. For cases "c" and "d", where the OOK channels have α=45 deg, the polarization rotation is observed around the SOP +45 and the constellations of the X and Y polarizations of the 16QAM channel are equally degraded by the polarization dependent XPM. We can observe an improvement after the CMA polarization recovery that rotates back the SOP of the PM-16QAM signal, nevertheless a residual penalty is still observed.

To further investigate the effects of XPM and XPolM, we increase the number of OOK channels

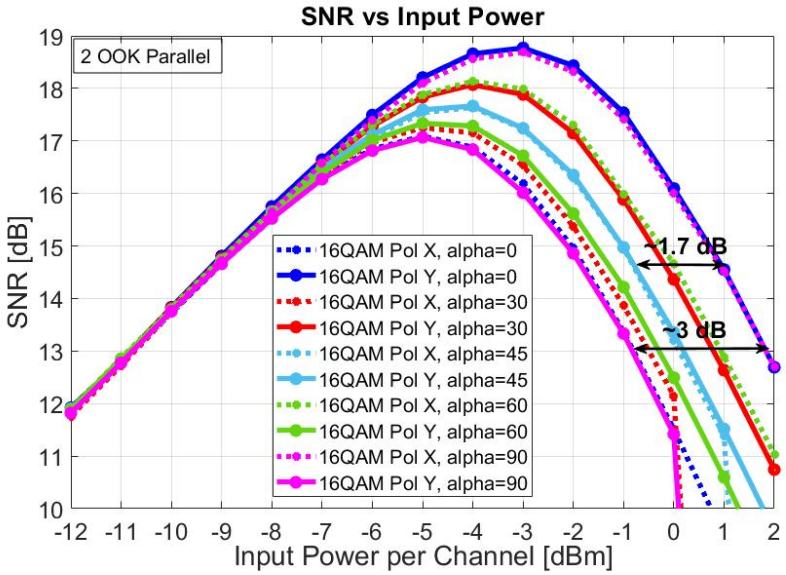

Fig. 3. 16QAM SNR versus Input power per channel with OOK neighbors at different polarization angles with respect to the polarization X of the coherent channel.

in our system to 8 and also compare to the case where a PM- Quadrature Phase Shift Keying (PM-QPSK) is used. In this simulation, the first OOK neighbor channels have 100 GHz separation to the channel under test and the subsequent OOK channels are 50GHz spaced to each other. Fig. 5 shows the SNR for each polarization and the average, for the 2 configurations where different alpha values and optical input powers were used. For the optical input powers, we choose the optimum input power and the cases with high and low nonlinearities. The results show that there is a small difference in SNR between QPSK and 16QAM modulation formats. At low input powers, the SNR dependence on the SOP of the OOK channels is low and increases with the input power. Furthermore, at high input powers we can observe that the average SNR is worst for the case where α=45 deg.

Funding

Please identify all appropriate funding sources by name and contract number. Funding information should be listed in a separate block preceding any acknowledgments. List only the funding agencies and any associated grants or project numbers, as shown in the example below:

National Science Foundation (NSF) (1253236, 0868895, 1222301); Program 973 (2014AA014402); Natural National Science Foundation (NSFC) (123456).

OSA participates in Crossref's Funding Data, a service that provides a standard way to report funding sources for published scholarly research. To ensure consistency, please enter any funding agencies and contract numbers from the Funding section in Prism during submission or revisions.

Acknowledgments

Acknowledgments, if included, should appear at the end of the document. The section title should not be numbered.

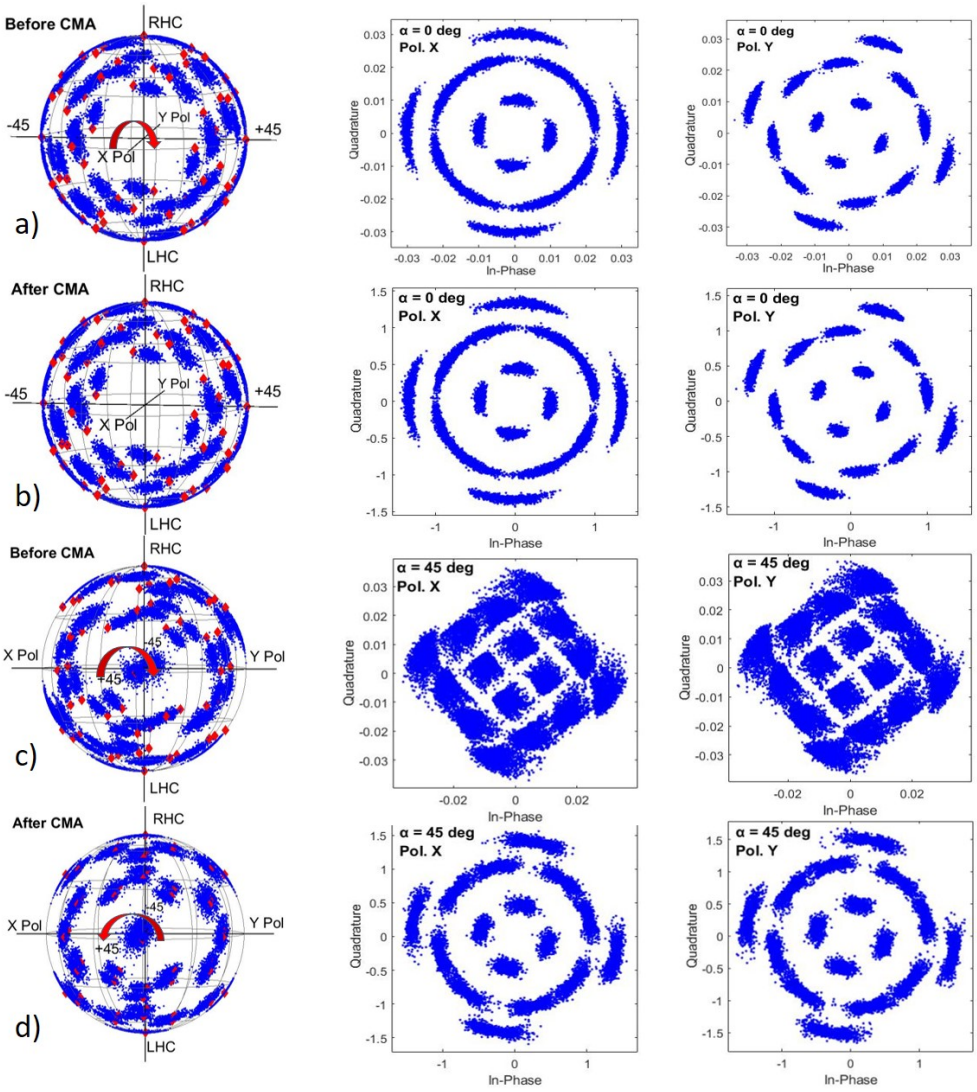

Fig. 4. SOP of the PM-16QAM signal at transmitter and receiver. Signal constellation in the receiver at an input power = -1 dBm, X and Y polarizations. a) Before CMA; α= 0 deg. b) After CMA; α= 0 deg. c) Before CMA; α= 45 deg. d) After CMA; α= 45 deg.

5. Conclusion

After proofreading the manuscript, compress your .tex manuscript file and all figures (which should be in EPS or PDF format) in a ZIP, TAR or TAR-GZIP package. All files must be referenced at the root level (e.g., file `figure-1.eps`, not `/myfigs/figure-1.eps`). If there are supplementary materials, the associated files should not be included in your manuscript archive but be uploaded separately through the Prism interface.

References

1. O. Vassilieva, T. Hoshida, X. Wang, J. Rasmussen, H. Miyata, and T. Naito, "Impact of polarization dependent loss and cross-phase modulation on polarization multiplexed dqpsk signals," in *OFC/NFOEC 2008 - 2008 Conference on Optical Fiber Communication/National Fiber Optic Engineers Conference,* (2008), pp. 1–3.

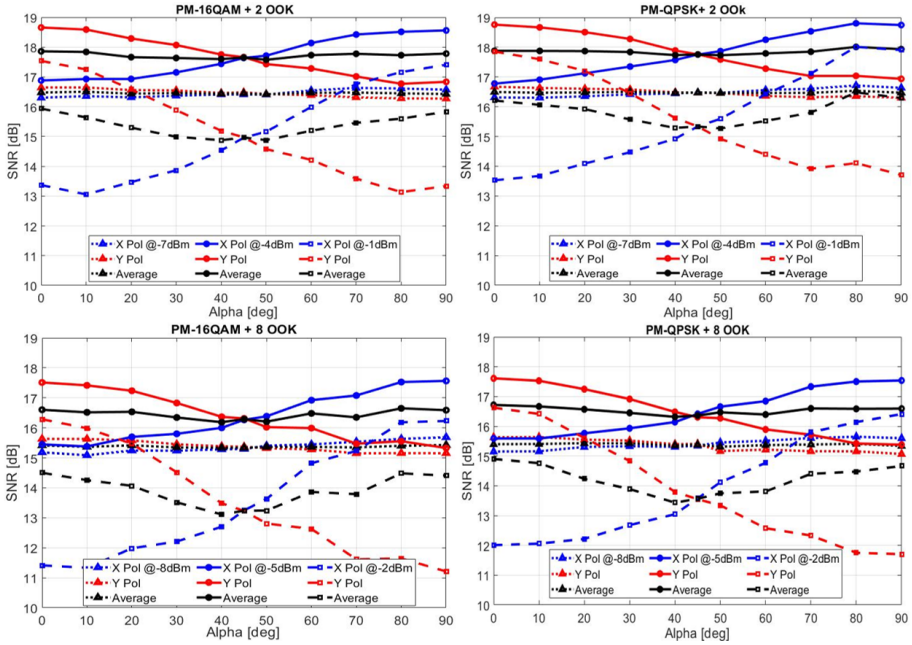

Fig. 5. Comparison between QPSK and 16QAM with 2 and 8 neighbor OOK channels in function of SNR vs Alpha for different Optical Input Powers

2. D. Rafique, M. Forzati, and J. MÃĕrtensson, "Impact of nonlinear fibre impairments in 112 gb/s pm-qpsk transmission with 43 gb/s and 10.7 gb/s neighbours," in *2010 12th International Conference on Transparent Optical Networks,* (2010), pp. 1–4.
3. E. Tipsuwannakul, M. N. Chughtai, M. Forzati, J. Mårtensson, P. Andrekson, and M. Karlsson, "Influence of self- and cross-phase modulation on 40 gbaud dual polarization dqpsk/d8psk signals in 10 gbit/s ook wdm systems," Opt. Express **18**, 24178–24188 (2010).
4. H. Louchet, A. Richter, I. Koltchanov, S. Mingaleev, N. Karelin, and K. Kuzmin, "Comparison of xpm and xpolm-induced impairments in mixed 10g âĂŞ 100g transmission," in *2011 13th International Conference on Transparent Optical Networks,* (2011), pp. 1–4.
5. M. N. Chughtai, M. Forzati, J. Mårtensson, and D. Rafique, "Influence of polarization state, baud rate and pmd on non-linear impairments in wdm systems with mixed pm (d)qpsk and ook channels," Opt. Express **20**, 8155–8160 (2012).
6. O. Bertran-Pardo, J. Renaudier, G. Charlet, H. Mardoyan, P. Tran, M. Salsi, and S. Bigo, "Overlaying 10 gb/s legacy optical networks with 40 and 100 gb/s coherent terminals," J. Light. Technol. **30**, 2367–2375 (2012).
7. M. Karlsson and H. Sunnerud, "Effects of nonlinearities on pmd-induced system impairments," J. Light. Technol. **24**, 4127–4137 (2006).
8. M. Karlsson, "Impact of cross-phase modulation in coherent transmission systems," in *IEEE Photonics Society Summer Topicals 2010,* (2010), pp. 127–128.
9. S. G. Evangelides, L. F. Mollenauer, J. P. Gordon, and N. S. Bergano, "Polarization multiplexing with solitons," J. Light. Technol. **10**, 28–35 (1992).
10. C. R. Menyuk and B. S. Marks, "Interaction of polarization mode dispersion and nonlinearity in optical fiber transmission systems," J. Light. Technol. **24**, 2806–2826 (2006).
11. L. F. Mollenauer, J. P. Gordon, and F. Heismann, "Polarization scattering by soliton–soliton collisions," Opt. Lett. **20**, 2060–2062 (1995).
12. A. Bononi, A. Vannucci, A. Orlandini, E. Corbel, S. Lanne, and S. Bigo, "Degree of polarization degradation due to cross-phase modulation and its impact on polarization-mode dispersion compensators," J. Light. Technol. **21**, 1903 (2003).
13. D. Wang and C. R. Menyuk, "Polarization evolution due to the kerr nonlinearity and chromatic dispersion," J. Light. Technol. **17**, 2520 (1999).
14. Q. Lin and G. P. Agrawal, "Effects of polarization-mode dispersion on cross-phase modulation in dispersion-managed wavelength-division-multiplexed systems," J. Light. Technol. **22**, 977 (2004).
15. M. Karlsson and M. Petersson, "Quaternion approach to pmd and pdl phenomena in optical fiber systems," J. Light. Technol. **22**, 1137 (2004).

16. J. P. Gordon and H. Kogelnik, “Pmd fundamentals: Polarization mode dispersion in optical fibers,” Proc. Natl. Acad. Sci. **97**, 4541–4550 (2000).